Inorganic Chemistry

Article

pubs.acs.org/IC

Rich Structural Chemistry in Scandium Selenium/Tellurium Oxides: Mixed-Valent Selenite−Selenates, $Sc_2(SeO_3)_2(SeO_4)$ and $Sc_2(TeO_3)(SeO_3)(SeO_4)$, and Ternary Tellurite, $Sc_2(TeO_3)_3$

Seung Yoon Song, Dong Woo Lee, and Kang Min Ok*

Department of Chemistry, Chung-Ang University, 84 Heukseok-ro, Dongjak-gu, Seoul 156-756, Republic of Korea

Supporting Information

ABSTRACT: Both single crystals and pure bulk phases of three new scandium selenium/tellurium oxides, $Sc_2(SeO_3)_2(SeO_4)$, $Sc_2(TeO_3)(SeO_3)(SeO_4)$, and $Sc_2(TeO_3)_3$, have been synthesized through hydrothermal and solid-state reactions. X-ray diffractions were used to determine the structures and confirm the phase purities of the reported materials. Isostructural $Sc_2(SeO_3)_2(SeO_4)$ and $Sc_2(TeO_3)(SeO_3)(SeO_4)$ reveal three-dimensional frameworks with ScO_7 pentagonal bipyramids, SeO_3 (and TeO_3) trigonal pyramids, and SeO_4 tetrahedra. A novel ternary scandium tellurite, $Sc_2(TeO_3)_3$, also shows a three-dimensional framework that is composed of ScO_6 octahedra, ScO_7-capped octahedra, and TeO_3 trigonal pyramids. All three materials accommodate local asymmetric coordination moieties owing to the lone pairs on Se^{4+} and Te^{4+} cations. The effect of coordination environments of constituent cations on the frameworks, dimensionalities, and centricities of products is discussed. Thorough characterizations including elemental analyses, infrared and UV−vis diffuse reflectance spectroscopies, thermal analyses, and dipole moment calculations for the reported materials are reported. Crystal data: $Sc_2(SeO_3)_2(SeO_4)$, monoclinic, space group $P2_1/c$ (No. 14), a = 6.5294(2) Å, b = 10.8557(4) Å, c = 12.6281(6) Å, β = 103.543(3)°, V = 870.21(6) Å^3, and Z = 4; $Sc_2(TeO_3)(SeO_3)(SeO_4)$, monoclinic, space group $P2_1/c$ (No. 14), a = 6.5345(12) Å, b = 10.970(2) Å, c = 12.559(2) Å, β = 102.699(10)°, V = 878.3(6) Å^3, and Z = 4; $Sc_2(TeO_3)_3$, monoclinic, space group $P2_1/n$ (No. 14), a = 5.2345(3) Å, b = 24.3958(15) Å, c = 6.8636(4) Å, β = 106.948(2)°, V = 838.42(9) Å^3, and Z = 4.

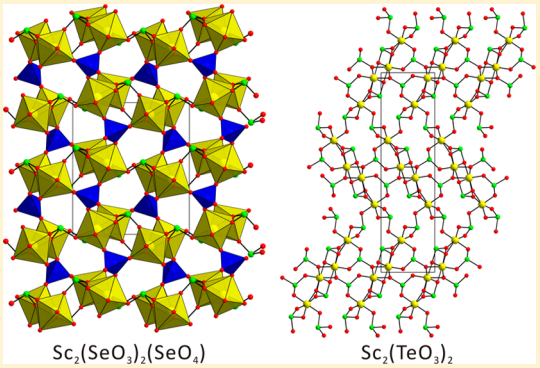

INTRODUCTION

A large number of materials with macroscopic noncentrosymmetric (NCS) crystal structures have been recently discovered from mixed-metal oxides containing two families of cations exhibiting local distorted coordination moieties, i.e., lone pair cations and d^0 transition metal elements.[1−10] The main distortive environments for both classes of cations are thought to be the result of electronic second-order Jahn−Teller (SOJT) effects.[11−16] In addition, the asymmetric units and variable coordination environments of the cations often result in rich structural frameworks when they are carefully combined.[17−26] Further structural variations would be also possible once the SOJT cations are united with p elements or halides, in which more flexible coordination capability or different tendency toward preferable elements, respectively, play important roles in completing a variety of framework architectures and dimensionalities.[27−31] In practice, selenium dioxide (SeO_2) and tellurium dioxide (TeO_2) are often introduced in the syntheses of new mixed-metal oxide materials with unsymmetrical structural backbones due to their excellent reactivities with other oxide reagents at lower reaction temperatures, great solubilities, and flexible coordination environments.[32−35] The ideas led us to explore new mixed-metal oxides accommodating Sc^{3+} and Se^{4+} (or Te^{4+}). During the initial hydrothermal reactions we were able to synthesize two mixed-valent selenite−selenate compounds, $Sc_2(SeO_3)_2(SeO_4)$ and $Sc_2(TeO_3)(SeO_3)(SeO_4)$, through redox reactions. On the other hand, solid-state reactions with similar starting materials resulted in a novel three-dimensional ternary mixed-metal scandium tellurite, $Sc_2(TeO_3)_3$. Richer structural chemistry has been observed from a variety of mixed-valent selenite−selenates, in which the structural variations are originated from the combination of SeO_4 terahedra and SeO_3 polyhedra in extended frameworks.[36−41] A NCS selenite−selenate such as $Au_2(SeO_3)_2(SeO_4)$ has also exhibited significant second-harmonic generation (SHG) efficiency attributable to the enhanced polarization from the lone electron pair.[42] Herein, we report detailed syntheses, structure determinations, and characterization of three new three-dimensional scandium selenium/tellurium oxides. Close structural examinations suggest that coordination environments of component cations strongly influence overall framework geometries, dimensionalities, and centricities. Thorough analyses including infrared and UV−vis diffuse reflectance spectra, thermal analyses, and dipole moment calculations will be presented.

Received: April 30, 2014
Published: June 11, 2014

   dx.doi.org/10.1021/ic501009c | Inorg. Chem. 2014, 53, 7040−7046

EXPERIMENTAL SECTION

Reagents. $Sc(NO_3)_3{\cdot}xH_2O$ (Acros, 99.9%), Sc_2O_3 (Alfa Aesar, 99.4%), SeO_2 (Aldrich, 98%), TeO_2 (Alfa Aesar, 98%), and H_2SeO_4 (Aldrich, 98%) were used as received.

Synthesis. $Sc_2(SeO_3)_2(SeO_4)$ and $Sc_2(TeO_3)(SeO_3)(SeO_4)$ were synthesized through hydrothermal reactions. For $Sc_2(SeO_3)_2(SeO_4)$, 0.249 g (1.00×10^{-3} mol) of $Sc(NO_3)_3{\cdot}xH_2O$, 0.222 g (2.00×10^{-3} mol) of SeO_2, and 2 mL of deionized water were combined. For $Sc_2(TeO_3)(SeO_3)(SeO_4)$, 0.249 g ($1.00 \times 10^{-3}$ mol) of $Sc(NO_3)_3{\cdot}xH_2O$, 0.080 g (5.00×10^{-4} mol) of TeO_2, 0.145 g (1.00×10^{-3} mol) of H_2SeO_4, 0.1 mL of HNO_3 (aq, 60 wt %), and 5 mL of deionized water were combined. Each reaction mixture was transferred into Teflon-lined Parr reactors. The reactors were sealed tightly and heated to 230 °C for 4 days. After cooling at a rate of 6 °C h^{-1} to room temperature, the autoclaves were opened and the reaction products were filtered and washed with distilled water. Pure products containing both colorless crystals and white polycrystalline materials were obtained in 50% and 28% yields for $Sc_2(SeO_3)_2(SeO_4)$ and $Sc_2(TeO_3)(SeO_3)(SeO_4)$, respectively, based on $Sc(NO_3)_3{\cdot}xH_2O$. Crystals and bulk polycrystalline samples of $Sc_2Te_3O_9$ were prepared through standard solid-state reactions. Single crystals of $Sc_2(TeO_3)_3$ were obtained by placing a mixture of a 0.138 g (1.00×10^{-3} mol) portion of Sc_2O_3, 0.233 g (5.00×10^{-4} mol) of Bi_2O_3, and 0.958 g (6.00×10^{-3} mol) of TeO_2 into a fused silica tube that was evacuated and subsequently sealed. The sealed tube containing reaction mixture was heated at 780 °C for 24 h and cooled slowly to room temperature at a rate of 6 °C h^{-1}. Colorless block crystals of $Sc_2(TeO_3)_3$ were grown with some unknown amorphous phases. After determining the crystal structure and exact stoichiometry, a pure bulk polycrystalline $Sc_2(TeO_3)_3$ was synthesized through a similar solid-state reaction. A stoichiometric mixture of Sc_2O_3 and TeO_2 was intimately ground and pressed into a pellet. The pellet was put into a fused quartz tube that was evacuated and sealed. The sealed tube was heated at 750 °C for 24 h and cooled to room temperature at a rate of 1 °C min^{-1}. A pure polycrystalline sample of $Sc_2Te_3O_9$ was successfully obtained, which was confirmed by powder X-ray diffraction.

Single-Crystal X-ray Diffraction. A standard crystallographic method was used to determine the crystal structures of the reported materials. A colorless block ($0.025 \times 0.038 \times 0.042$ mm^3) for $Sc_2(SeO_3)_2(SeO_4)$, a colorless needle ($0.011 \times 0.012 \times 0.075$ mm^3) for $Sc_2(TeO_3)(SeO_3)(SeO_4)$, and a colorless block ($0.024 \times 0.031 \times 0.051$ mm^3) for $Sc_2(TeO_3)_3$ were used for single-crystal data analyses. Diffraction data were obtained at room temperature using a Bruker SMART BREEZE diffractometer equipped with a 1K CCD area detector using graphite-monochromated Mo Kα radiation. A hemisphere of data was collected using a narrow-frame method with an exposure time of 10 s/frame and scan widths of 0.30° in omega. At the end of data collection, the first 50 frames were remeasured in order to monitor crystal and instrument stability. The maximum correction applied to the intensities was less than 1%. The SAINT program was used to integrate the diffraction data,[43] in which the intensities were corrected for air absorption, polarization, Lorentz factor, and absorption attributed to the variation in the path length through the detector faceplate. The SADABS program was used to make absorption correction on the diffraction data.[44] Data were solved using SHELXS-97[45] and refined with SHELXL-97.[46] Displacement parameters for all atoms were refined anisotropically and converged for $I > 2\sigma(I)$. All calculations were performed using the WinGX-98 crystallographic software package.[47] Crystallographic data for $Sc_2(SeO_3)_2(SeO_4)$, $Sc_2(TeO_3)(SeO_3)(SeO_4)$, and $Sc_2(TeO_3)_3$ are listed in Table 1. The slightly higher $R_w(F_o^2)$ value for $Sc_2(TeO_3)(SeO_3)(SeO_4)$ compared to other reported crystals may be attributable to the weaker diffraction arising from the needle-like morphology.

Powder X-ray Diffraction. Powder X-ray diffraction data were obtained on a Bruker D8-Advance diffractometer using Cu Kα radiation at room temperature with 40 kV and 40 mA. The well-ground polycrystalline samples were mounted on sample holders and scanned in the 2θ range from 10° to 70° with a step size of 0.02° and a step time of 0.2 s. Powder XRD patterns for the reported materials are in good agreements with the calculated data from the single-crystal model.

Table 1. Crystallographic Data for $Sc_2(SeO_3)_2(SeO_4)$, $Sc_2(TeO_3)(SeO_3)(SeO_4)$, and $Sc_2(TeO_3)_3$

formula	$Sc_2Se_3O_{10}$	$Sc_2TeSe_2O_{10}$	$Sc_2Te_3O_9$
fw	486.80	535.44	616.72
space group	$P2_1/c$ (No. 14)	$P2_1/c$ (No. 14)	$P2_1/n$ (No. 14)
a (Å)	6.5294(2)	6.5345(12)	5.2345(3)
b (Å)	10.8557(4)	10.970(2)	24.3958(15)
c (Å)	12.6281(6)	12.559(2)	6.8636(4)
β (deg)	103.543(3)	102.699(10)	106.948(2)
V (Å^3)	870.21(6)	878.3(3)	838.42(9)
Z	4	4	4
T (°C)	298.0(2)	298.0(2)	298.0(2)
λ (Å)	0.710 73	0.710 73	0.710 73
ρ_{calcd} (g cm^{-3})	3.716	4.049	4.886
μ (mm^{-1})	14.146	13.128	11.876
$R(F)^a$	0.0489	0.0587	0.0182
$R_w(F_o^2)^b$	0.0628	0.1663	0.0362

$^aR(F) = \Sigma \; ||F_o| - |F_c|| / \Sigma \; |F_o|$. $^bR_w(F_o^2) = [\Sigma w(F_o^2 - F_c^2)^2 / \Sigma w(F_o^2)^2]^{1/2}$.

Vibrational Spectroscopy. Infrared spectra were recorded on a Thermo Scientific Nicolet 6700 FT-IR spectrometer in the range of 400−4000 cm^{-1} with the samples embedded in KBr matrixes.

UV−vis Spectroscopy. UV−vis diffuse reflectance spectral data were obtained at room temperature on a Varian Cary 500 scan UV−vis−NIR spectrophotometer equipped with a double-beam photomultiplier tube in the range of 200−2500 nm at the Korea Photonics Technology Institute. The Kubelka−Munk function was used to convert the reflectance spectra to the absorbance data.[48,49]

Thermogravimetric Analysis. Thermal analyses were carried out on a Setaram LABSYS thermogravimetric analyzer. Polycrystalline samples were contained within alumina crucibles and heated from room temperature to 1000 °C at a rate of 10 °C min^{-1} under flowing argon.

Scanning Electron Microscope (SEM)/Energy-Dispersive Analysis by X-ray (EDAX). SEM/EDAX analyses have been performed using a Hitachi S-3400N/Horiba Energy EX-250 instruments. EDAX for $Sc_2(SeO_3)_2(SeO_4)$, $Sc_2(TeO_3)(SeO_3)(SeO_4)$, and $Sc_2(TeO_3)_3$ reveal Sc:Se, Sc:Te:Se, and Sc:Te ratios of approximately 2.0:3.1, 2.1:0.8:2.0, and 2.0:3.2, respectively.

RESULTS AND DISCUSSION

Syntheses. Both hydrothermal and solid-state reactions were used to prepare new scandium selenium/tellurium oxides materials. $Sc_2(SeO_3)_2(SeO_4)$ and $Sc_2(TeO_3)(SeO_3)(SeO_4)$ were synthesized under hydrothermal reaction conditions. While $Sc_2(SeO_3)_2(SeO_4)$ was prepared through the oxidation reaction of $Se^{4+}O_2$ in the presence of a nitrate, $Sc(NO_3)_3{\cdot}xH_2O$, $Sc_2(TeO_3)(SeO_3)(SeO_4)$ was obtained by reduction of $H_2Se^{6+}O_4$ during hydrothermal reactions. A number of mixed-valent selenite−selenate compounds have been synthesized through similar redox reactions under hydrothermal reaction conditions.[39,50−53] However, no redox reactions occurred during preparation of $Sc_2(TeO_3)_3$, since the material was prepared by a solid-state reaction in vacuum.

Structures. *$Sc_2(SeO_3)_2(SeO_4)$ and $Sc_2(TeO_3)(SeO_3)(SeO_4)$.* $Sc_2(SeO_3)_2(SeO_4)$ and $Sc_2(TeO_3)(SeO_3)(SeO_4)$ are isostructural and crystallize in the centrosymmetric monoclinic space group, $P2_1/c$ (No. 14). Thus, only the structural details of $Sc_2(SeO_3)_2(SeO_4)$ will be described here. The structure of $Sc_2(SeO_3)_2(SeO_4)$ consists of ScO_7 pentagonal bipyramids, $Se^{4+}O_3$ trigonal pyramids, and $Se^{6+}O_4$ tetrahedra (see Figure 1).

dx.doi.org/10.1021/ic501009c | Inorg. Chem. 2014, 53, 7040−7046

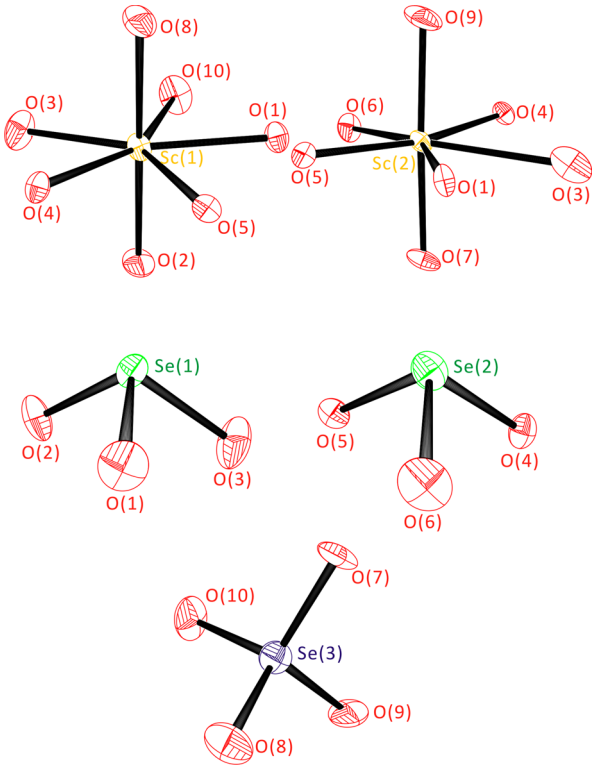

Figure 1. ORTEP (50% probability ellipsoids) drawings representing the coordination moieties of Sc^{3+}, Se^{4+}, and Se^{6+} in $Sc_2(SeO_3)_2(SeO_4)$.

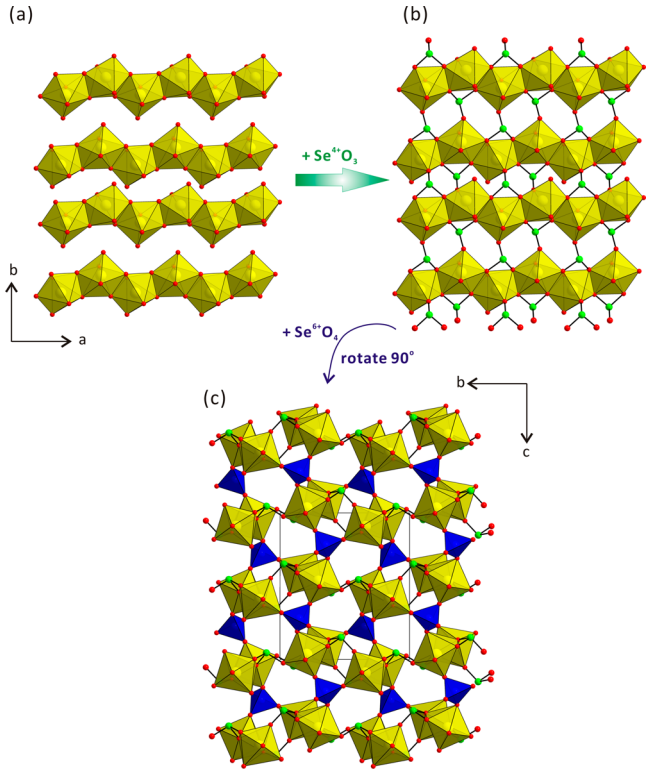

Figure 2. Ball-and-stick and polyhedral representations of (a) chains of edge-shared ScO_7 pentagonal bipyramids along the [100] direction, (b) corrugated layers formed by connection of SeO_3 groups in the *ab* plane, and (c) a three-dimensional framework generated by linking of SeO_4 tetrahedra in the *bc* plane for $Sc_2(SeO_3)_2(SeO_4)$ (blue, Se^{6+}; green, Se^{4+}, dark yellow, Sc^{3+}; red, O).

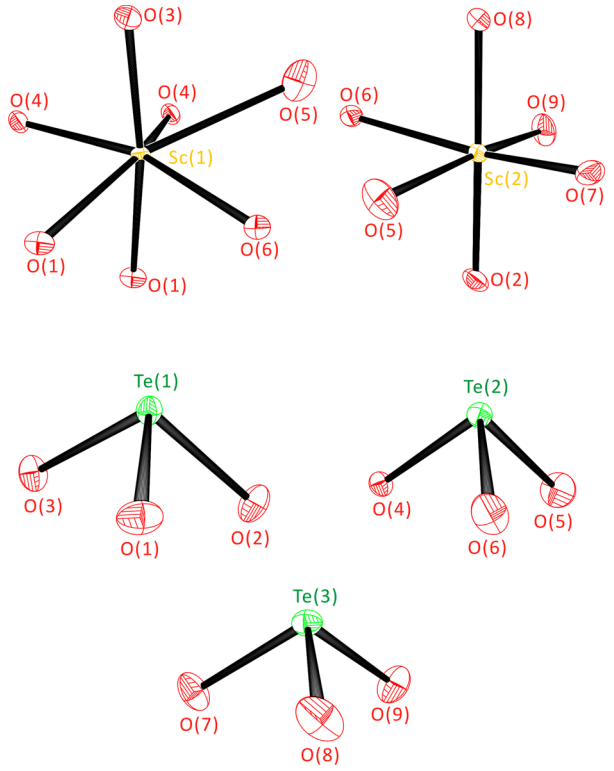

Figure 3. ORTEP (50% probability ellipsoids) drawings representing the coordination moieties of Sc^{3+} and Te^{4+} in $Sc_2(TeO_3)_2$.

Both unique $Sc(1)^{3+}$ and $Sc(2)^{3+}$ cations are connected to seven oxygen atoms and exhibit distorted ScO_7 pentagonal bipyramidal geometry. While the $Sc(1)^{3+}$ cations show seven intermediate Sc(1)−O bond distances that are ranging from 2.034(7) to 2.267(6) Å, the $Sc(2)^{3+}$ cations reveal six intermediate bond lengths [2.074(8)−2.143(6) Å] and one very long [2.567(7) and 2.817(15) Å for $Sc_2(TeO_3)(SeO_3)(SeO_4)$] Sc(2)−O bond length. Two unique Se^{4+} cations containing stereochemically active lone pairs are found in asymmetrically distorted SeO_3 trigonal-pyramidal moieties. Se^{4+}−O bond distances range from 1.648(7) to 1.717(6) Å, and O−Se^{4+}−O bond angles range from 90.3(3)° to 104.6(3)°. Finally, within an asymmetric unit, a unique Se^{6+} cation exists in a slightly distorted $Se^{6+}O_4$ tetrahedral coordination environment. While the Se^{6+}−O bond lengths range from 1.619(7) to 1.652(7) Å, the O−Se^{6+}−O bond angles range from 107.1(3)° to 113.7(4)°.

$Sc(1)O_7$ and $Sc(2)O_7$ pentagonal bipyramids share their edges through O(1), O(3), O(4), and O(5) and form infinite unidimensional chains along the [100] direction (see Figure 2a). Similar infinite chains consisting of edge-shared pentagonal bipyramids have been previously reported from a uranyl oxide fluoride and a scandium selenite materials.[26,54] The chains are then connected by $Se^{4+}O_3$ groups along [001] and [00−1] through O(1), O(2), O(3), O(4), O(5), and O(6), which generates a corrugated layer in the *ab* plane (see Figure 2b). Here the asymmetric $Se^{4+}O_3$ groups act as interchain linkers. In fact, the very long bond distance of Sc(2)−O(3) is attributable to this connection of the $Se(1)O_3$ linker maintaining the chain structure. The lone pairs on the Se^{4+} direct approximately to the [001] and [00−1] directions. The layers are further linked by $Se^{6+}O_4$ tetrahedra through O(7), O(8), O(9), and O(10) along the [001] direction, which creates a three-dimensional

dx.doi.org/10.1021/ic501009c | *Inorg. Chem.* 2014, 53, 7040−7046

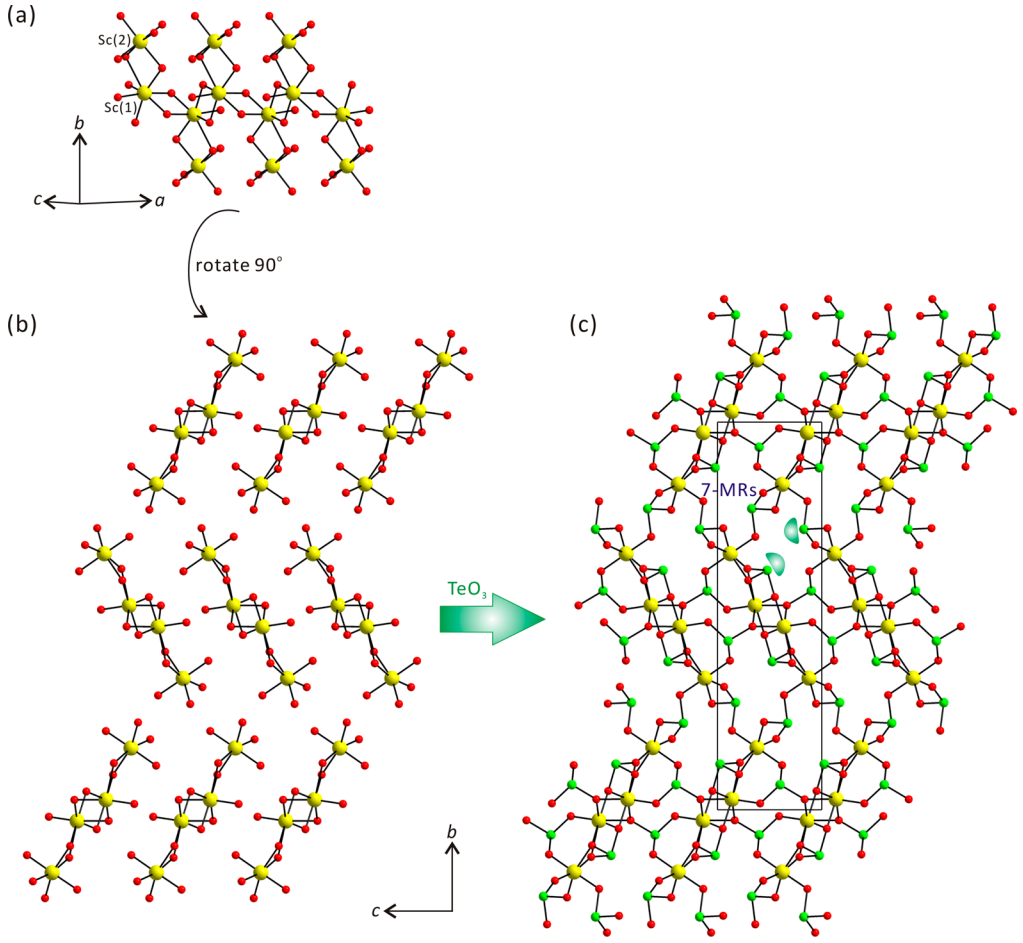

Figure 4. Ball-and-stick models of (a) infinite chains constructed by edge-shared $Sc(1)O_7$-capped octahedra and $Sc(2)O_6$ octahedra (a) along the [100] direction, (b) infinite zigzag bands in the *bc* plane, and (c) a three-dimensional framework obtained by linking of TeO_3 linkers in the *bc* plane for $Sc_2(TeO_3)_2$ (green, Te^{4+}, dark yellow, Sc^{3+}; red, O). Note that seven-membered rings (7-MRs) channels consisting of ScO_6, ScO_7, and TeO_3 are observed within the framework, and the lone pairs on the Te^{4+} cations point toward inside the channels.

framework structure (see Figure 2c). The framework structure of $Sc_2(SeO_3)_2(SeO_4)$ may be represented as a neutral backbone of $\{2[Sc^{3+}O_{3/2}O_{4/3}]^{-2.667}\ 2[Se^{4+}O_{1/2}O_{2/3}]^{+1.667}\ [Se^{6+}O_{4/2}]^{+2}\}^0$. Bond valence sums[55,56] for Sc^{3+}, Se^{4+}, Se^{6+}, and O^{2-} can be calculated to be 3.06−3.09, 4.06−4.10, 6.06, and 1.93−2.13, respectively.

$Sc_2(TeO_3)_3$. $Sc_2(TeO_3)_3$ is a new ternary scandium tellurite that is crystallizing in the monoclinic space group $P2_1/n$ (No. 14) with a three-dimensional framework consisting of ScO_6, ScO_7, and TeO_3 groups (see Figure 3). The $Sc(1)^{3+}$ cations are in capped octahedral moieties with seven oxygen atoms, whereas the $Sc(2)^{3+}$ cations are in distorted octahedral coordination environments with only six oxygen atoms. While the $Sc(1)^{3+}$ cations show six intermediate [2.053(3)−2.193(3) Å] bond lengths and one very long [2.584(3) Å] Sc(1)−O bond length, the $Sc(2)^{3+}$ cations exhibit six normal Sc(2)−O bonds that range from 2.033(3) to 2.246(3) Å. Also, within an asymmetric unit three unique Te^{4+} cations exist and reveal TeO_3 trigonal pyramidal coordination environments. The observed Te−O bond lengths and O−Te−O bond angles are 1.849(3)−1.905(2) Å and 86.12(13)−102.83(13)°, respectively.

Each $Sc(1)O_7$-capped octahedron shares its edges through O(1) and O(4) and generates chains approximately along the [100] direction (see Figure 4a). Also, $Sc(2)O_6$ distorted octahedra further share their edges with $Sc(1)O_7$ polyhedra through O(5) and O(6) approximately along the [010] and [0−10] directions, which results in infinite zigzag bands along the [100] direction (see Figure 4b). The bands are linked by TeO_3 groups, and a three-dimensional framework structure is completed by the linkers (see Figure 4c). More specifically, whereas the $Te(1)O_3$ and $Te(3)O_3$ groups serve as interband linkers, the $Te(2)O_3$ groups function as intraband linkers. Similar to $Sc_2(SeO_3)_2(SeO_4)$, the very long Sc(1)−O(5) bond length is attributed to this linking of $Te(2)O_3$ groups in order to maintain the zigzag band. Within the framework, seven-membered rings (7-MRs) channels composed of ScO_6, ScO_7, and TeO_3 are observed and the lone pairs on the Te^{4+} cations point to inside the channels. The structure of $Sc_2(TeO_3)_3$ is also delineated as a neutral 3D framework of $\{[Sc(1)^{3+}O_{1/2}O_{6/3}]^{-2}\ [Sc(2)^{3+}O_{4/2}O_{2/3}]^{-2.333}\ [Te(1)^{4+}O_{2/2}O_{1/3}]^{+1.333}\ [Te(2)^{4+}O_{3/3}]^{+2}\ [Te(3)^{4+}O_{3/2}]^{+1}\}^0$ in connectivity terms. Bond valence sums[55,56] are calculated to be 2.91−2.97, 3.97−3.99, and 1.90−2.09 for Sc^{3+}, Te^{4+}, and O^{2-}, respectively.

Effect of Coordination Environments of Cations on Framework Structures, Dimensionalities, and Centricities. The isostructural $Sc_2(SeO_3)_2(SeO_4)$ and $Sc_2(TeO_3)(SeO_3)(SeO_4)$ are stoichiometrically similar to a couple of known mixed-valent selenium oxides, $Bi_2(SeO_3)_2(SeO_4)$[57] and $Au_2(SeO_3)_2(SeO_4)$.[42] However, all of the selenite−selenate materials exhibit completely different framework structures and

dx.doi.org/10.1021/ic501009c | *Inorg. Chem.* 2014, 53, 7040−7046

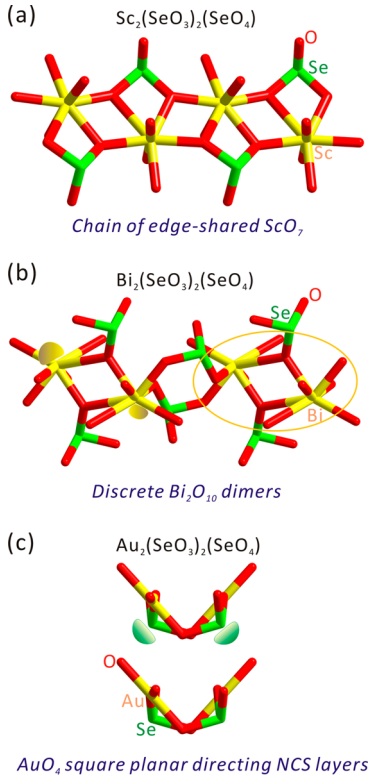

Figure 5. Wire models representing how coordination environments of constituent cations influence overall framework structures, dimensionalities, and centricities. (a) Unidimensional chains of edge-shared ScO_7 groups, (b) discrete Bi_2O_{10} dimers, and (c) electronically preferable AuO_4 square planar are observed from $Sc_2(SeO_3)_2(SeO_4)$, $Bi_2(SeO_3)_2(SeO_4)$, and $Au_2(SeO_3)_2(SeO_4)$, respectively.

Table 2. Infrared Vibrations (cm^{-1}) for $Sc_2(SeO_3)_2(SeO_4)$, $Sc_2(TeO_3)(SeO_3)(SeO_4)$, and $Sc_2(TeO_3)_3$

Sc–O	Se^{4+}–O or Te^{4+}–O	Se^{6+}–O
	$Sc_2(SeO_3)_2(SeO_4)$	
428	528	412
486	543	894
	686	925
	740	968
	806	
$Sc_2(TeO_3)(SeO_3)(SeO_4)$		
434	542	413
486	681	895
	735	924
	806	962
$Sc_2(TeO_3)_3$		
432	542	
496	559	
	627	
	650	
	708	
	735	
	783	
	802	
	837	

dimensionalities. More close structural analyses suggest that the coordination environments of constituent cations strongly influence overall framework geometries. In $Sc_2(SeO_3)_2(SeO_4)$ and $Sc_2(TeO_3)(SeO_3)(SeO_4)$, relatively smaller Sc^{3+} (0.745 Å) cations[58] reveal ScO_7 distorted pentagonal bipyramidal coordination moieties with seven oxygen atoms, which can generate unidimensional chains of edge-shared ScO_7 groups (see Figure 5a). With $Bi_2(SeO_3)_2(SeO_4)$, however, discrete Bi_2O_{10} dimers are obtained attributed to the larger cation size of Bi^{3+} (1.17 Å)[58] along with lone pairs (see Figure 5b). Although all three materials have 3D frameworks through the connections of SeO_3 and SeO_4 linkers, it is obvious that the local coordination environment of constituent cations and their orientation significantly effect on the extended frameworks. Meanwhile, $Au_2(SeO_3)_2(SeO_4)$ contains Au^{3+} cation in a square planar coordination moiety, which is a prototype structure for d^8 cations (see Figure 5c). Here, the electronically preferable AuO_4 square planar geometry and SeO_3 connectors with lone pairs direct a layered structure with a macroscopic NCS space group.

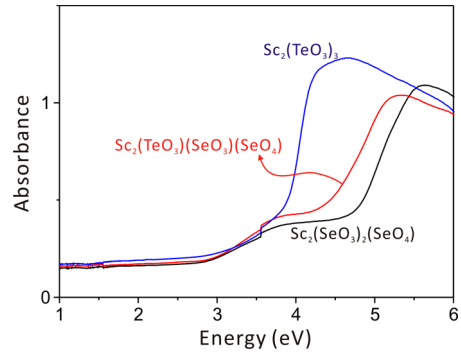

Figure 6. UV–vis diffuse reflectance spectra of $Sc_2(SeO_3)_2(SeO_4)$, $Sc_2(TeO_3)(SeO_3)(SeO_4)$, and $Sc_2(TeO_3)_3$ revealing the absorption edges at 4.4, 4.0, and 3.7 eV, respectively.

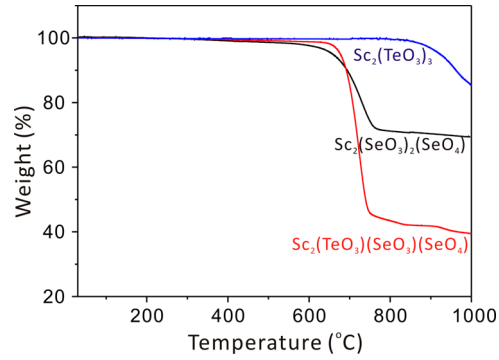

Figure 7. Thermogravimetric analyses diagrams of $Sc_2(SeO_3)_2(SeO_4)$, $Sc_2(TeO_3)(SeO_3)(SeO_4)$, and $Sc_2(TeO_3)_3$. Upon heating, $Sc_2(SeO_3)_2(SeO_4)$, $Sc_2(TeO_3)(SeO_3)(SeO_4)$, and $Sc_2(TeO_3)_3$ are thermally stable up to 600, 630, and 820 °C, respectively.

Table 3. Summary of the Dipole Moments for SeO_3 and TeO_3 Polyhedra (D = Debyes)

compound	species	dipole moment (D)
$Sc_2(SeO_3)_2(SeO_4)$	$Se(1)O_3$	9.11
	$Se(2)O_3$	9.10
$Sc_2(TeO_3)(SeO_3)(SeO_4)$	$Te(1)O_3$	11.79
	$Se(1)O_3$	8.65
$Sc_2(TeO_3)_3$	$Te(1)O_3$	9.07
	$Te(2)O_3$	10.06
	$Te(3)O_3$	8.64

dx.doi.org/10.1021/ic501009c | Inorg. Chem. 2014, 53, 7040–7046

Spectroscopic Characterizations. Infrared spectra for $Sc_2(SeO_3)_2(SeO_4)$, $Sc_2(TeO_3)(SeO_3)(SeO_4)$, and $Sc_2(TeO_3)_3$ reveal characteristic bands for Sc−O, Se−O, and Te−O vibrations. Several bands occurring in the region of around 405−496 cm^{-1} can be assigned to the Sc−O vibration. The peaks attributed to Se^{4+}−O and/or Te^{4+}−O vibrations are observed at around 542−837 cm^{-1}. The bands occurring around 410 and 894−968 cm^{-1} can be assigned to Se^{6+}−O vibrations. The infrared vibrations and assignments for the reported materials are summarized in Table 2. The assignments are consistent with those previously reported compounds.[59−62]

The UV−vis diffuse reflectance spectra for all three reported materials have been obtained, and the absorption (K/S) data have been calculated from the following Kubelka−Munk function[48,49]

$$F(R) = \frac{(1-R)^2}{2R} = \frac{K}{S}$$

where S is the scattering, K is the absorption, and R is the reflectance. Extrapolations of the linear parts of the rising curves to zero revealed dominant absorptions at 4.4, 4.0, and 3.7 eV for $Sc_2(SeO_3)_2(SeO_4)$, $Sc_2(TeO_3)(SeO_3)(SeO_4)$, and $Sc_2(TeO_3)_3$, respectively, in the (K/S) versus E plots (see Figure 6). The values are consistent with the white colors of the materials. The assigned direct band gaps for the reported materials may be due to the degree of Sc (3d) orbitals involved in the conduction bands and the distortions arising from SeO_3, SeO_4, or TeO_3 polyhedra.

Thermal Analysis. In order to investigate the thermal stabilities of the reported materials, thermogravimetric analyses (TGA) have been performed (see Figure 7). TGA analyses reveal that $Sc_2(SeO_3)_2(SeO_4)$, $Sc_2(TeO_3)(SeO_3)(SeO_4)$, and $Sc_2(TeO_3)_3$ are stable up to 600, 630, and 820 °C, respectively, upon heating. Above the temperatures, the materials thermally decompose to mixtures of Sc_2O_3 (PDF-#741210) and some unknown amorphous phases, which is identified by powder XRD measurements. XRD patterns of thermally decomposed products for all three materials are deposited in the Supporting Information.

Dipole Moment Calculations. The reported materials hold lone pair cations such as Se^{4+} and Te^{4+} within their frameworks, although they all crystallize in centrosymmetric space groups. Thus, it is worth understanding the asymmetric coordination environments of the lone pair cations by determining the local dipole moments of the polyhedra. The direction and extent of the distortions in SeO_3 and TeO_3 groups can be quantified through the calculations. Using the methodology published before,[63−65] the local dipole moments for SeO_3 and TeO_3 in $Sc_2(SeO_3)_2(SeO_4)$, $Sc_2(TeO_3)(SeO_3)(SeO_4)$, and $Sc_2(TeO_3)_3$ are calculated to be about 8.65−9.11 and 8.64−11.79 D (D = Debyes), respectively. The calculated dipole moments are consistent with those previously reported values.[10,29,66,67] Calculations of local dipole moments are listed in Table 3.

CONCLUSIONS

Three new scandium selenium/tellurium oxides materials, $Sc_2(SeO_3)_2(SeO_4)$, $Sc_2(TeO_3)(SeO_3)(SeO_4)$, and $Sc_2(TeO_3)_3$, have been successfully synthesized by hydrothermal and solid-state reactions. Whereas redox reactions occurred during the hydrothermal syntheses of $Sc_2(SeO_3)_2(SeO_4)$ and $Sc_2(TeO_3)(SeO_3)(SeO_4)$, the oxidation states of the starting materials for the synthesis of $Sc_2(TeO_3)_3$ remained the same during the solid-state reaction in vacuum. Isostructural $Sc_2(SeO_3)_2(SeO_4)$ and $Sc_2(TeO_3)(SeO_3)(SeO_4)$ exhibit three-dimensional frameworks with ScO_7 pentagonal bipyramids, $Se^{4+}O_3$ or $Te^{4+}O_3$ trigonal pyramids, and $Se^{6+}O_4$ tetrahedra. Another three-dimensional ternary oxide, $Sc_2(TeO_3)_3$, contains ScO_6 octahedra, ScO_7-capped octahedra, and TeO_3 trigonal pyramids. Rich structural chemistry found in the new mixed-metal oxides materials is mainly attributable to the coordination environments of constituent cations. Spectroscopic characterizations including IR and UV−vis diffuse reflectance spectroscopies, thermal analyses, and dipole moment calculations have been also reported.

ASSOCIATED CONTENT

Supporting Information

X-ray crystallographic file in CIF format, calculated and observed X-ray diffraction patterns, infrared spectra, and XRD patterns for the calcined products for $Sc_2(SeO_3)_2(SeO_4)$, $Sc_2(TeO_3)(SeO_3)(SeO_4)$, and $Sc_2(TeO_3)_3$. This material is available free of charge via the Internet at http://pubs.acs.org.

AUTHOR INFORMATION

Corresponding Author

*Phone: +82-2-820-5197. Fax: +82-2-825-4736. E-mail: kmok@cau.ac.kr.

Notes

The authors declare no competing financial interest.

ACKNOWLEDGMENTS

This research was supported by the Basic Science Research Program through the National Research Foundation of Korea (NRF) funded by the Ministry of Education, Science & Technology (grant 2013R1A2A2A01007170).

REFERENCES

(1) Ra, H.-S.; Ok, K. M.; Halasyamani, P. S. *J. Am. Chem. Soc.* **2003**, *125*, 7764−7765.
(2) Kim, J.-H.; Baek, J.; Halasyamani, P. S. *Chem. Mater.* **2007**, *19*, 5637−5641.
(3) Chang, H. Y.; Kim, S.-H.; Halasyamani, P. S.; Ok, K. M. *J. Am. Chem. Soc.* **2009**, *131*, 2426−2427.
(4) Chang, H.-Y.; Kim, S.-H.; Ok, K. M.; Halasyamani, P. S. *J. Am. Chem. Soc.* **2009**, *131*, 6865−6873.
(5) Chang, H. Y.; Kim, S. W.; Halasyamani, P. S. *Chem. Mater.* **2010**, *22*, 3241−3250.
(6) Yang, B.; Hu, C.; Xu, X.; Sun, C.; Zhang Jian, H.; Mao, J.-G. *Chem. Mater.* **2010**, *22*, 1545−1550.
(7) Lee, D. W.; Oh, S. J.; Halasyamani, P. S.; Ok, K. M. *Inorg. Chem.* **2011**, *50*, 4473−4480.
(8) Sun, C.-F.; Hu, C.-L.; Xu, X.; Yang, B.-P.; Mao, J.-G. *J. Am. Chem. Soc.* **2011**, *133*, 5561−5572.
(9) Oh, S.-J.; Lee, D. W.; Ok, K. M. *Inorg. Chem.* **2012**, *51*, 5393−5399.
(10) Kim, Y. H.; Lee, D. W.; Ok, K. M. *Inorg. Chem.* **2014**, *53*, 1250−1256.
(11) Opik, U.; Pryce, M. H. L. *Proc. R. Soc. London* **1957**, *A238*, 425−447.
(12) Bader, R. F. W. *Can. J. Chem.* **1962**, *40*, 1164−1175.
(13) Pearson, R. G. *J. Am. Chem. Soc.* **1969**, *91*, 4947−4955.
(14) Pearson, R. G. *J. Mol. Struct.: THEOCHEM* **1983**, *103*, 25−34.
(15) Wheeler, R. A.; Whangbo, M.-H.; Hughbanks, T.; Hoffmann, R.; Burdett, J. K.; Albright, T. A. *J. Am. Chem. Soc.* **1986**, *108*, 2222−2236.
(16) Kunz, M.; Brown, I. D. *J. Solid State Chem.* **1995**, *115*, 395−406.

(17) Champarnaud-Mesjard, J. C.; Frit, B.; Chagraoui, A.; Tairi, A. *Z. Anorg. Allg. Chem.* **1996**, *622*, 1907−1912.
(18) Wedel, B.; Mueller-Buschbaum, H. *Z. Naturforsch. B: J. Chem. Sci.* **1996**, *51*, 1411−1414.
(19) Blanchandin, S.; Champarnaud-Mesjard, J. C.; Thomas, P.; Frit, B. *Solid State Sci.* **2000**, *2*, 223−228.
(20) Ok, K. M.; Halasyamani, P. S. *Inorg. Chem.* **2002**, *41*, 3805−3807.
(21) Ok, K. M.; Halasyamani, P. S. *Angew. Chem., Int. Ed.* **2004**, *43*, 5489−5491.
(22) Ok, K. M.; Halasyamani, P. S. *Inorg. Chem.* **2005**, *44*, 3919−3925.
(23) Li, P. X.; Kong, F.; Hu, C. L.; Zhao, N.; Mao, J.-G. *Inorg. Chem.* **2010**, *49*, 5943−5952.
(24) Zhang, S.-Y.; Hu, C.-L.; Sun, C.-F.; Mao, J.-G. *Inorg. Chem.* **2010**, *49*, 11627−11636.
(25) Oh, S.-J.; Lee, D. W.; Ok, K. M. *Dalton Trans.* **2012**, *41*, 2995−3000.
(26) Kim, Y. H.; Lee, D. W.; Ok, K. M. *Inorg. Chem.* **2013**, *52*, 11450−11456.
(27) Zhang, D.; Berger, H.; Kremer, R. K.; Wulferding, D.; Lemmens, P.; Johnsson, M. *Inorg. Chem.* **2010**, *49*, 9683−9688.
(28) Zhang, D.; Kremer, R. K.; Lemmens, P.; Choi, K.-Y.; Liu, J.; Whangbo, M.-H.; Berger, H.; Skourski, Y.; Johnsson, M. *Inorg. Chem.* **2011**, *50*, 12877−12885.
(29) Lee, D. W.; Kim, S. B.; Ok, K. M. *Inorg. Chem.* **2012**, *51*, 8530−8537.
(30) Lee, D. W.; Ok, K. M. *Inorg. Chem.* **2012**, *52*, 5176−5184.
(31) Zimmermann, I.; Kremer, R. K.; Reuvekamp, P.; Johnsson, M. *Dalton Trans.* **2013**, *42*, 8815−8819.
(32) Ok, K. M.; Halasyamani, P. S. *Chem. Mater.* **2002**, *14*, 2360−2364.
(33) Lide, D. R. *CRC Handbook of Chemistry and Physics*, Internet Version 2005; CRC Press: Boca Raton, FL, 2005.
(34) Shen, Y. L.; Jiang, H. L.; Xu, J.; Mao, J.-G.; Cheah, K. W. *Inorg. Chem.* **2005**, *44*, 9314−9321.
(35) Lee, D. W.; Ok, K. M. *Inorg. Chem.* **2013**, *52*, 6236−6238.
(36) Effenberger, H. *Mineral. Petrol.* **1987**, *36*, 3−12.
(37) Baran, J.; Lis, T.; Marchewka, M.; Ratajczak, H. *J. Mol. Struct.* **1991**, *250*, 13−45.
(38) Giester, G. *Monatsh. Chem.* **1992**, *123*, 957−963.
(39) Morris, R. E.; Wilkinson, A. P.; Cheetham, A. K. *Inorg. Chem.* **1992**, *31*, 4774−4777.
(40) Harrison, W. T. A.; Zhang, Z. *Eur. J. Solid State Inorg. Chem.* **1997**, *34*, 599−606.
(41) Weil, M.; Kolitsch, U. *Acta Crystallogr., Sect. C* **2002**, *C58*, i47−i49.
(42) Wickleder, M. S.; Buchner, O.; Wickleder, C.; Sheik, S. e.; Brunklaus, G.; Eckert, H. *Inorg. Chem.* **2004**, *43*, 5860−5864.
(43) *SAINT, Program for Area Detector Absorption Correction*, version 4.05; Siemens Analytical X-ray Instruments: Madison, WI, 1995.
(44) Blessing, R. H. *Acta Crystallogr., Sec. A: Found. Crystallogr.* **1995**, *A51*, 33−38.
(45) Sheldrick, G. M. *SHELXS-97-A program for automatic solution of crystal structures*; University of Goettingen: Goettingen, Germany, 1997.
(46) Sheldrick, G. M. *SHELXL-97-A program for crystal structure refinement*; University of Goettingen: Goettingen, Germany, 1997.
(47) Farrugia, L. J. *J. Appl. Crystallogr.* **1999**, *32*, 837−838.
(48) Kubelka, P.; Munk, F. *Z. Technol. Phys.* **1931**, *12*, 593.
(49) Tauc, J. *Mater. Res. Bull.* **1970**, *5*, 721−729.
(50) Berdonosov, P. S.; Schmidt, P.; Dityat'yev, O. A.; Dolgikh, V. A.; Lightfoot, P.; Ruck, M. *Z. Anorg. Allg. Chem.* **2004**, *630*, 1395−1400.
(51) Feng, M.-L.; Mao, J.-G. *J. Alloys Compd.* **2005**, *388*, 23−27.
(52) Sullens, T. A.; Almond, P. M.; Byrd, J. A.; Beitz, J. V.; Bray, T. H.; Albrecht-Schmitt, T. E. *J. Solid State Chem.* **2006**, *179*, 1192−1201.
(53) Ling, J.; Albrecht Schmitt, T. E. *J. Solid State Chem.* **2007**, *180*, 1601−1607.
(54) Ok, K. M.; Doran, M. B.; O'Hare, D. *J. Mater. Chem.* **2006**, *16*, 3366−3368.
(55) Brown, I. D.; Altermatt, D. *Acta Crystallogr.* **1985**, *B41*, 244−247.
(56) Brese, N. E.; O'Keeffe, M. *Acta Crystallogr.* **1991**, *B47*, 192−197.
(57) Lee, E. P.; Song, S. Y.; Lee, D. W.; Ok, K. M. *Inorg. Chem.* **2013**, *52*, 4097−4103.
(58) Shannon, R. D. *Acta Crystallogr.* **1976**, *A32*, 751−767.
(59) Baran, J.; Marchewka, M. K.; Ratajczak, H. *J. Mol. Struct.* **1997**, *436*−*437*, 257−279.
(60) Johnston, M. G.; Harrison, W. T. A. *J. Solid State Chem.* **2004**, *177*, 4316−4324.
(61) Akama, Y.; Sawada, T.; Ueda, T. *J. Mol. Struct.* **2005**, *750*, 44−50.
(62) Zhang, S.-Y.; Hu, C.-L.; Li, P.-X.; Jiang, H.-L.; Mao, J.-G. *Dalton Trans.* **2012**, *41*, 9532−9542.
(63) Galy, J.; Meunier, G. *J. Solid State Chem.* **1975**, *13*, 142−159.
(64) Maggard, P. A.; Nault, T. S.; Stern, C. L.; Poeppelmeier, K. R. *J. Solid State Chem.* **2003**, *175*, 27−33.
(65) Izumi, H. K.; Kirsch, J. E.; Stern, C. L.; Poeppelmeier, K. R. *Inorg. Chem.* **2005**, *44*, 884−895.
(66) Kim, M. K.; Jo, V.; Lee, D. W.; Ok, K. M. *Dalton Trans.* **2010**, *39*, 6037−6042.
(67) Lee, D. W.; Ok, K. M. *Solid State Sci.* **2010**, *12*, 2036−2041.